

A MEASUREMENT OF THE PHASES OF THE CP -VIOLATING AMPLITUDES IN $K^0 \rightarrow 2\pi$ DECAYS AND A TEST OF CPT INVARIANCE

R. CAROSI, P. CLARKE ¹, D. COWARD ^{2,3}, D. CUNDY, N. DOBLE, L. GATIGNON, V. GIBSON, P. GRAFSTRÖM, R. HAGELBERG, G. KESSELER, J. VAN DER LANS, H.N. NELSON, H. WAHL
CERN, CH-1211 Geneva 23, Switzerland

R. BLACK, D.J. CANDLIN, J. MUIR, K.J. PEACH
Physics Department, University of Edinburgh, Edinburgh EH9 3J2, UK

H. BLÜMER, R. HEINZ, M. KASEMANN ⁴, K. KLEINKNECHT, P. MAYER, B. PANZER, B. RENK, S. ROEHN, H. ROHRER
Institut für Physik, Universität Mainz, D-6500 Mainz, FRG ⁵

E. AUGÉ, R.L. CHASE, D. FOURNIER, P. HEUSSE, L. ICONOMIDOU-FAYARD, I. HARRUS, A.M. LUTZ, A.C. SCHAFFER
Laboratoire de l'Accélérateur Linéaire, Université de Paris-Sud, F-91405 Orsay, France ⁶

L. BERTANZA, A. BIGI, P. CALAFIURA, M. CALVETTI ⁷, R. CASALI, C. CERRI, R. FANTECHI, G. GARGANI, I. MANNELLI ⁸, A. NAPPI, G.M. PIERAZZINI
Dipartimento di Fisica and Sezione dell'INFN, I-56010 Pisa, Italy

C. BECKER, H. BURKHARDT, M. HOLDER, G. QUAST ⁴, M. ROST, H.G. SANDER ⁹, W. WEIHS and G. ZECH
Fachbereich Physik, Universität Siegen, D-5900 Siegen, FRG ¹⁰

Received 21 December 1989

The phases of the CP -violating amplitudes in $K^0 \rightarrow \pi^+ \pi^-$ and $K^0 \rightarrow 2\pi^0$ decays, $\phi_{+-} = 46.9^\circ \pm 2.2^\circ$ and $\phi_{00} = 47.1^\circ \pm 2.8^\circ$, have been measured in the same experiment, and a direct comparison gives the phase difference $\phi_{00} - \phi_{+-} = 0.2^\circ \pm 2.9^\circ$. This result leads to an upper limit on possible CPT violation in the K^0 mass matrix, of $|(m_{\bar{K}^0} - m_{K^0})/m_{K^0}| < 5 \times 10^{-18}$ at the 95% confidence level and is the most stringent test of the equality of particle and antiparticle masses.

¹ Present address: Brunel, The University of West London, Uxbridge UB8 3PH, UK.

² On leave from SLAC, Stanford, CA 94305, USA.

³ Work supported in part by the US Department of Energy under contract DE-AC03-76SF00515.

⁴ present address: CERN, CH-1211 Geneva 23, Switzerland.

⁵ Funded by the German Federal Minister for Research and Technology (BMFT) under contract 054Mz18.

⁶ Funded by Institut National de Physique des Particules et de Physique Nucléaire, France.

⁷ Present address: Dipartimento di Fisica and Sezione dell'INFN, I-06100 Perugia, Italy.

⁸ Present address: Scuola Normale Superiore, I-56100 Pisa, Italy.

⁹ Present address: Universität Mainz, D-6500 Mainz, FRG.

¹⁰ Funded by the German Federal Minister for Research and Technology (BMFT) under contract 054Si74.

1. Introduction

The violation of *CP* symmetry is well established in the neutral kaon system and can be accommodated within the standard model [1,2]. *CPT* invariance, however, is usually assumed [3,4] and implies a violation of *T* invariance which is consistent with existing data [5,6]. A consequence of *CPT* symmetry is that the mass and the lifetime of a particle and its antiparticle are equal. The neutral-kaon system provides a sensitive test of *CPT* due to the small mass difference between the short- and long-lived K^0 states [7],

$$m_L - m_S = (3.522 \pm 0.016) \times 10^{-15} \text{ GeV},$$

which gives a reference against which the $K^0 - \bar{K}^0$ mass difference can be measured.

The interference of *CP*-violating $K^0 \rightarrow 2\pi$ decays with *CP*-conserving $K^0 \rightarrow 2\pi$ decays provides a unique tool for the study of *CP*- and *CPT*-violating effects in the neutral-kaon system. It is convenient to define the *CP* eigenstates

$$K_1 = \frac{1}{\sqrt{2}} (K^0 + \bar{K}^0) \quad \text{with } CP = +1,$$

$$K_2 = \frac{1}{\sqrt{2}} (K^0 - \bar{K}^0) \quad \text{with } CP = -1.$$

The physical particles are the mass eigenstates and can be written as

$$K_S \approx K_1 + (\epsilon + \delta)K_2 \quad \text{and} \quad K_L \approx K_2 + (\epsilon - \delta)K_1,$$

where ϵ is a measure of the *CP* violation induced by kaon-state mixing, and δ allows *CP* violation with *CPT* non-conservation [5,6,8]. With the convention $\text{Im} A_0 = 0$ [9], the phase of ϵ is given by unitarity [10] to be

$$\phi_\epsilon \approx \tan^{-1} 2 \frac{m_L - m_S}{\Gamma_S} = 43.7^\circ \pm 0.2^\circ.$$

Violation of *CP* may also occur in the decay of the $K_2 \rightarrow \pi\pi$ with a relative amplitude of ϵ' ,

$$\epsilon' = \frac{i}{\sqrt{2}} \text{Im} \left(\frac{A_2}{A_0} \right) \exp[i(\delta_2 - \delta_0)],$$

where A_0 and A_2 are the amplitudes for the decay into isospin 0 and 2 two-pion states. Evidence for direct *CP* violation has recently been reported by this col-

laboration [11]. Assuming *CPT* invariance, the phase of ϵ' is determined by the difference in the s-wave $\pi\pi$ scattering phase shifts, δ_0 and δ_2 , for the isospin 0 and 2 states, respectively. A compendium of the measured phase shifts gives $\phi_{\epsilon'}$ in the range $45^\circ \pm 15^\circ$ [12].

The *CP*-violation parameters η_{+-} and η_{00} are defined as the respective ratios of the *CP*-violating and *CP*-allowed amplitudes for the K_L and K_S decays into two charged and two neutral pions. The relevant experimental quantities are the magnitudes and phases of η_{+-} and η_{00} :

$$\eta_{+-} = \frac{\langle \pi^+ \pi^- | T | K_L \rangle}{\langle \pi^+ \pi^- | T | K_S \rangle} = |\eta_{+-}| \exp(i\phi_{+-}),$$

$$\eta_{00} = \frac{\langle \pi^0 \pi^0 | T | K_L \rangle}{\langle \pi^0 \pi^0 | T | K_S \rangle} = |\eta_{00}| \exp(i\phi_{00}).$$

The amplitude ratios have contributions from *CP* violation in the kaon-state mixing (ϵ) and from direct *CP* violation in the $K_2 \rightarrow 2\pi$ decay (ϵ'), and can be written to a good approximation as

$$\eta_{+-} = \epsilon + \epsilon', \quad \eta_{00} = \epsilon - 2\epsilon'.$$

The status of the *CP*-violation parameters from previous experimental results is given in table 1. The magnitude of η_{+-} is obtained from direct measurements of the amplitude ratio using the time-dependent rate of interfering $K_S \rightarrow \pi^+ \pi^-$ and $K_L \rightarrow \pi^+ \pi^-$ decays, and from measurements of branching ratios of $K_L \rightarrow \pi^+ \pi^-$ to three-body decay modes. The value of $|\eta_{00}/\eta_{+-}|$ is taken from the most precise measurements, and the phases ϕ_{+-} and ϕ_{00} are evaluated from published data using the current average value of the

Table 1
Experimental status of the *CP*-violation parameters, the K_S and K_L lifetimes and their mass difference prior to this experiment.

Parameter	Mean value	References
$ \eta_{+-} $	$(2.272 \pm 0.021) \times 10^{-3}$	13,15,16
$ \eta_{00}/\eta_{+-} $	0.990 ± 0.003	11,17
ϕ_{+-} [deg]	45.6 ± 1.4	14,15,18
ϕ_{00} [deg]	55.7 ± 5.9	19
τ_S [s]	$(0.8922 \pm 0.0020) \times 10^{-10}$	13,18,20
τ_L [s]	$(5.15 \pm 0.04) \times 10^{-8}$	21
Δm [\hbar s ⁻¹]	$(0.5351 \pm 0.0024) \times 10^{10}$	7

K_L - K_S mass difference. The relevant references [7,11,13-21] are given in the table.

The magnitude of $\epsilon'/\epsilon = (3.3 \pm 1.0) \times 10^{-3}$ and the phases of ϵ and ϵ' suggest that the magnitudes and the phases of η_{+-} and η_{00} are close to those of ϵ . In fact, one would expect the phase difference $\phi_{00} - \phi_{+-}$ to be less than 0.2° if CPT is conserved. Experimentally, both η_{+-} and η_{00} have magnitudes approximately equal to the magnitude of ϵ , and the phase ϕ_{+-} is in reasonable agreement with ϕ_ϵ . However, a measurement of ϕ_{00} by Christenson et al. shows a 2 standard deviation discrepancy [19]. A direct comparison with ϕ_{+-} in the same experiment gives $\phi_{00} - \phi_{+-} = 12.6^\circ \pm 6.2^\circ$. Given that $\phi_{+-} \approx \phi_\epsilon$, such a large phase difference, if confirmed, would imply CPT violation in both the kaon-state mixing and the decay.

Consequently, a dedicated experiment to measure the phases ϕ_{+-} and ϕ_{00} has been performed at the CERN Super Proton Synchrotron (SPS). The phases of the CP -violation parameters η_{+-} and η_{00} were determined from the time dependence of the rate of kaon decays into two pions:

$$I_{2\pi}(t) = S(p) \left\{ \exp\left(-\frac{t}{\tau_S}\right) + |\eta|^2 \exp\left(-\frac{t}{\tau_L}\right) + 2D(p) |\eta| \exp\left[-\frac{t}{2}\left(\frac{1}{\tau_S} + \frac{1}{\tau_L}\right)\right] \cos(\Delta m t - \phi) \right\},$$

where t is the time in the kaon rest system after incoherent K^0 and \bar{K}^0 production by strong interactions, and $S(p)$ is the production spectrum of $K^0 + \bar{K}^0$ as a function of momentum. The dilution factor, $D(p)$, is a measure of the initial admixture of K^0 and \bar{K}^0 , namely $D(p) = (K^0 - \bar{K}^0)/(K^0 + \bar{K}^0)$; τ_S and τ_L are the lifetimes of K_S and K_L , and $\Delta m = m_L - m_S$ is their mass difference.

The type of beam and target arrangement was chosen such as to obtain the maximum acceptance in the interference region, at about 12 K_S lifetimes. Two target stations were employed: one near to the detector (K_{near}) and one far from the detector (K_{far}). For this arrangement, the acceptance correction is negligible if the phases are determined from the ratio of lifetime distributions for the two target positions. At the average kaon momentum of about 100 GeV/c, at which one K_S lifetime corresponds to 5 m, the dis-

tance between the two targets, 14.4 m, corresponds to a phase shift of about 75° .

2. Experimental set-up and data-taking

The detector was the same as that used in the ϵ'/ϵ measurement [11,22], but the beam layout was modified substantially to provide K_L and K_S with maximum sensitivity to the interference region. Kaons of mean momentum around 100 GeV/c are produced from a 450 GeV/c proton beam focused to intercept either of the two targets at a downward inclination of 3.6 mrad with respect to the kaon beamline. Both targets are constructed from beryllium, and are 40 cm in length and 2 mm in diameter. Proton intensities of $\sim 1.4 \times 10^{10}$ (K_{near}) and $\sim 2 \times 10^{10}$ (K_{far}) per pulse were selected and the neutral beams were defined by a two-stage collimation system. Each target is followed, 10 m downstream, by a collimator of 2.8 mm radius to define the angular acceptance of the beam. Mobile collimators with radii of 1.4 cm and 2.1 cm, located at a distance of 33.6 m and 48 m from the K_{near} and K_{far} targets respectively, remove the background from the defining collimator.

The apparatus is shown in fig. 1 and a full description is given in ref. [22]. Kaons that decay along 50 m in an evacuated tank are detected further downstream at about 120 m from the final collimator. Decays into charged and neutral pions are detected concurrently. The principal features of the charged and neutral pion detection can be summarized as follows:

- Charged pion decays: $K^0 \rightarrow \pi^+ \pi^-$.
 - two wire chambers, with ± 0.5 mm resolution in each projection, spaced 25 m apart in a helium enclosure, measure the direction and lateral position of charged pions;
 - A hodoscope of scintillation counters triggers on $\pi^+ \pi^-$ decays by a coincidence of hits in opposite quadrants;
 - an iron/scintillator sandwich calorimeter, in conjunction with the liquid-argon calorimeter, measures the energy of charged pions with $\pm 65\%/\sqrt{E}$ (GeV) resolution;
 - two planes of scintillators, after a total of 3 m of iron equivalent, reject $K_L \rightarrow \pi \mu \nu$ decays.
- Neutral pion decays: $K^0 \rightarrow 2\pi^0 \rightarrow 4\gamma$,
 - a liquid-argon/lead sandwich calorimeter with strip

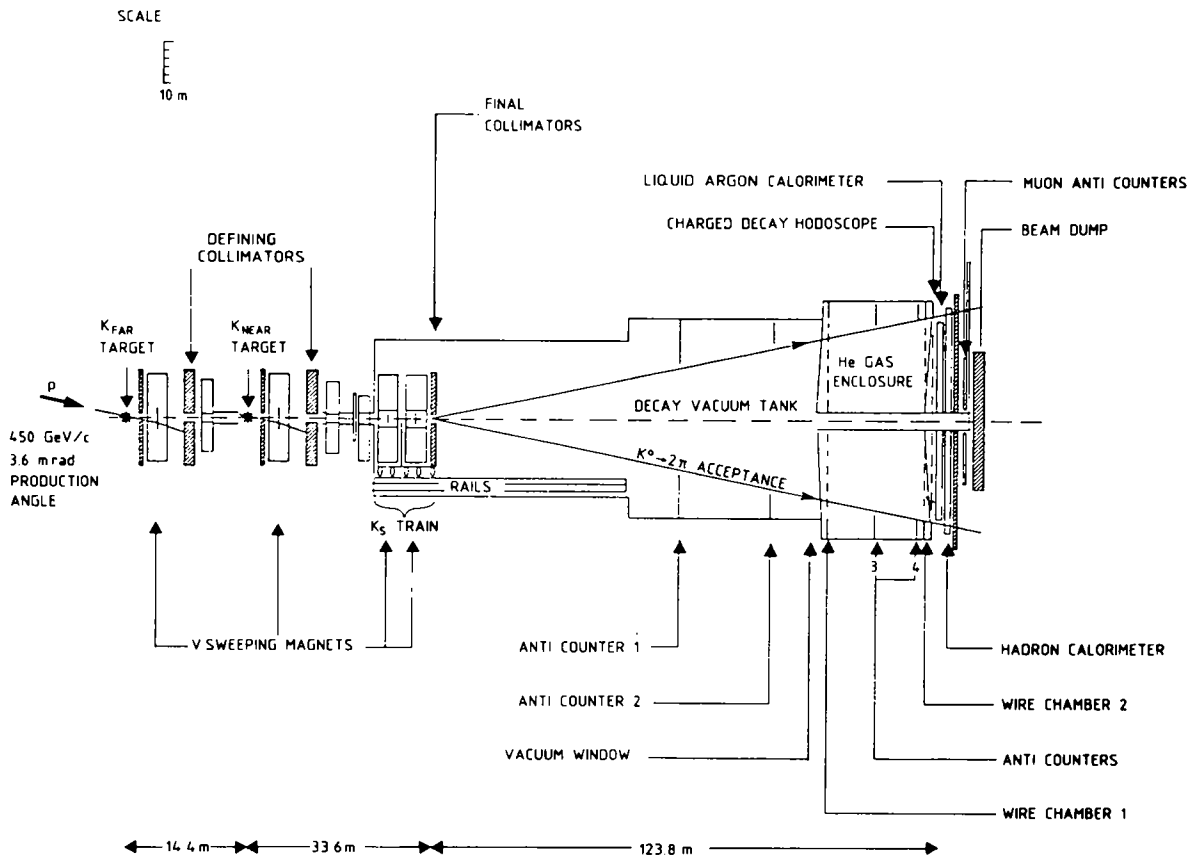


Fig. 1. Schematic layout of the beam and detector.

readout measures photons with a ± 0.5 mm position resolution and an energy resolution attributed to shower fluctuations $[\pm 7.5\%/\sqrt{E} \text{ (GeV)}]$, uniformity of response ($\pm 0.5\%$) and noise (± 0.1 GeV);

- a plane of scintillation counters, installed in the liquid argon after 13 radiation lengths of material, triggers on neutral decays;
- four ring-shaped anticounters surrounding the decay region detect large-angle photons and thus reduce the $K_L \rightarrow 3\pi^0$ and $K_L \rightarrow \pi^+ \pi^- \pi^0$ charged background.

The trigger for two-body K^0 decays is applied in three stages. A pretrigger signal is generated by the combination of a coincidence in either of the two scintillation counter hodoscopes and by the absence of a veto in any of the anticounters. The trigger is accepted if further conditions regarding the calorimeter energies, the number of wire chamber hits, and the number of clusters in the liquid-argon calorimeter are

satisfied. The final on-line data reduction is achieved by two computer processors. These decrease the number of events accepted, whose calculated lifetimes from the production target are less than 7 K_S lifetimes, and thus increase the proportion of events accepted in the interference region. The down-scaling factors were chosen to give about the same number of events per K_S lifetime.

Data were taken over a period of approximately 70 days during 1987. Typically, every eight hours, the beam was interchanged between the two target stations. For the purpose of the energy scale calibration, pure K_S data from a mobile target were also taken at the centre and at the most upstream end of the decay region after each data-taking cycle. A total of 144×10^6 triggers were written to tape at a rate of ~ 1000 events per burst.

3. Charged reconstruction and background

The $K^0 \rightarrow \pi^+ \pi^-$ decays are reconstructed from the measured space points in the wire chambers and the track energies in the calorimeters. The longitudinal vertex position is calculated from the extrapolation of the tracks in the wire chambers and has a resolution better than 1 m. The kaon energy is calculated with typically 1% precision from the kaon mass, the

opening angle between the two tracks, and the ratio of the track energies:

$$E_K = \frac{1}{\theta} \sqrt{(2 + 1/R + R) [m_K^2 - m_\pi^2 (2 + 1/R + R)]},$$

where R is the ratio of the two pion energies measured in the calorimeter. A cut on $R < 2.5$ excludes contamination from $\Lambda \rightarrow p\pi$ decays. The energy scale is determined entirely from the wire chamber geometry and is independent of the energy scale of the calorimeter, provided that any non-linearities are small. A cut on the closest distance of approach of the two tracks at the approximate vertex position, an invariant-mass cut around the kaon mass, and a centre-of-gravity cut guarantee a selection of good events.

Three-body K_L decays contribute to the charged background. Events with identified isolated photons, such as $K_L \rightarrow \pi^+ \pi^- \pi^0$, are easily rejected. Most $K_L \rightarrow \pi e \nu$ decays are identified and rejected by comparing, for each track, the energy deposited in the front half of the electromagnetic calorimeter with the total energy. The $K_L \rightarrow \pi \mu \nu$ decays are rejected by the muon vetos. The residual background is subtracted from the shape of the d_t distribution. The distance d_t is the perpendicular distance from the target to the decay plane, and its shape is determined from a sample of $K_L \rightarrow \pi e \nu$ decays. The d_t distributions for K_{near} and K_{far} are shown in fig. 2. The background is extrapolated from the region $6 < d_t < 10$ cm and subtracted in the signal region. Background events constitute 0.01% for K_{near} and 0.05% for K_{far} of the total data samples. The total charged-background subtraction has the effect of reducing ϕ_{+-} by 0.2° .

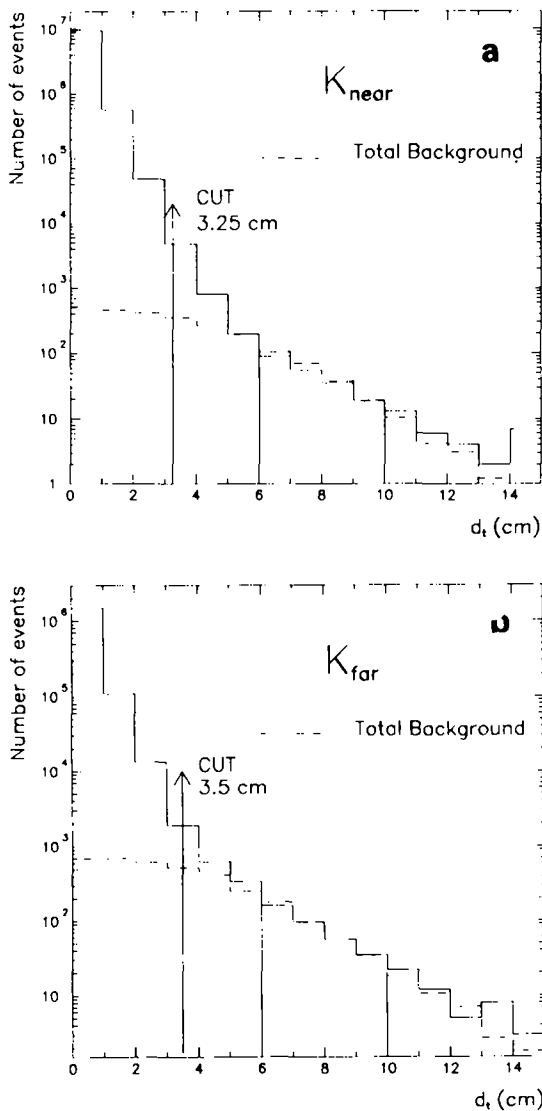


Fig. 2. Event distributions for charged decays as a function of d_t , with signal and background regions indicated.

4. Neutral reconstruction and background

The $K^0 \rightarrow 2\pi^0 \rightarrow 4\gamma$ decays are reconstructed from the measured energy and positions of the four photons in the liquid-argon calorimeter. The kaon mass is used as a constraint in the computation of the distance of the decay vertex, z , from the position of the calorimeter, z_{cal} :

$$z = z_{cal} - \frac{1}{m_K} \sqrt{\sum_{i,j < i}^4 E_i E_j [(x_i - x_j)^2 + (y_i - y_j)^2]}.$$

The kaon energy and its longitudinal vertex position

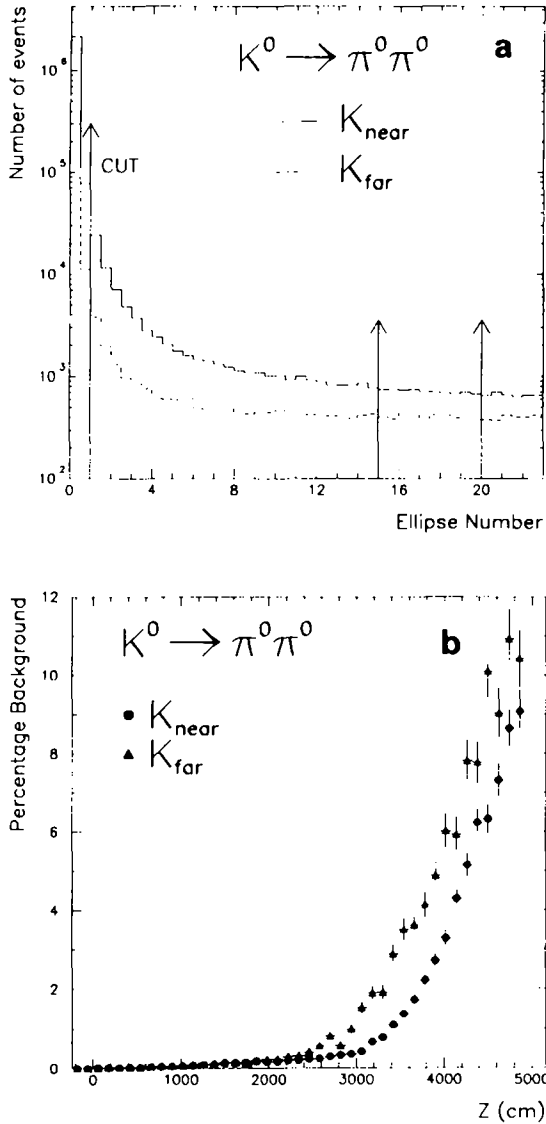


Fig. 3. The number of accepted 4γ events as a function of ellipse number, and the percentage of background as a function of decay vertex for neutral events.

are measured typically with 1% accuracy. Events are accepted if the energy of each photon is greater than 5 GeV and there is at least 5 cm separation between the shower centres. The centre of gravity of the energies of all photons must lie within the beam region.

The background to $2\pi^0$ decays is predominantly due to $K_L \rightarrow 3\pi^0$ decays where two of the photons have es-

caped detection. Since the reconstructed decay vertex of these background events appears shifted towards the calorimeter, 80% of this background is removed by requiring that the decay vertex is within 50 m from the beginning of the decay region. The background is uniformly distributed in a two-dimensional scatter plot of the two-photon invariant masses. The π^0 mass resolution is typically 2 MeV. Signal and background events are counted in ellipses of equal area around the $2\pi^0$ peak [11,23]. Events are selected in the central ellipse, and the background is subtracted by a flat extrapolation into the signal region from the outer ellipses (see fig. 3a). The amount of background subtracted, 0.06% for K_{near} and 0.26% for K_{far} , is different because of the relative number of K_L and K_S decays in each beam. The percentage background subtracted as a function of the position of the decay vertex is shown in fig. 3b. The total effect of the neutral background subtraction on the result is to reduce ϕ_{00} by 0.6° .

A change in the energy scale of the calorimeter has the effect of also shifting the vertex position of the

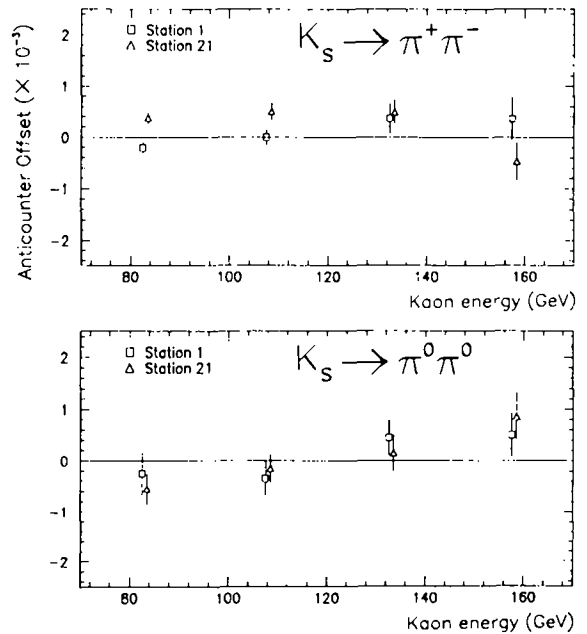


Fig. 4. The relative offset of the reconstructed K_S anticounter position as a function of the kaon momentum for charged and neutral decays for upstream (station 1) and mid-decay region (station 21) decays.

decay, thus changing the calculated lifetime from the target. An uncertainty of 10^{-3} in the energy scale is equivalent to an error of 1° on the phase. The absolute energy scale is determined from a fit of the vertex distribution to the known position of the anticounter in the K_S beam with the technique described in ref. [11]. An accuracy of 10^{-3} in the energy scale is equivalent to a 10 cm position uncertainty at the centre of the decay volume. A comparison of the offset in the reconstructed K_S anticounter position as a function of kaon momentum for charged and neutral decays is shown in fig. 4.

5. Analysis and results

The number of events after all cuts and in the ranges

$1.2 < z < 49.2$ m and $70 < E_K < 170$ GeV, are given in table 2. The $2.1 \times 10^6 K^0 \rightarrow 2\pi^0$ events correspond to 3000 $K_L \rightarrow 2\pi^0$ events per K_S lifetime in the interference region. Qualitative evidence for the interference between the K_S and K_L decay amplitudes is demonstrated in fig. 5, which shows the rate of decay of kaons

Table 2
Event statistics. The numbers in brackets include the lifetime down-scaling factors.

	$K^0 \rightarrow \pi^0 \pi^0 (\times 10^6)$	$K^0 \rightarrow \pi^+ \pi^- (\times 10^6)$
K_{near}	1.81 (2.24)	2.24 (5.99)
K_{far}	0.31 (0.31)	0.57 (0.84)

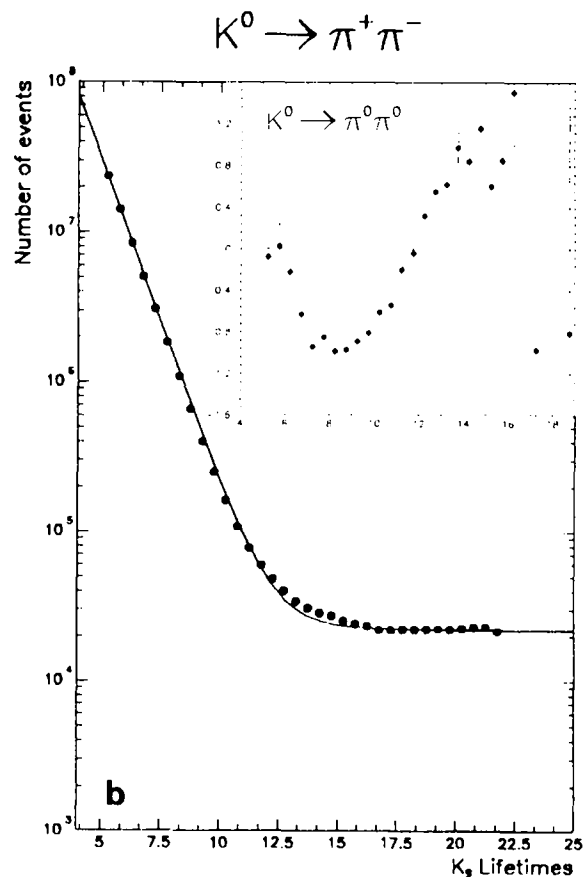
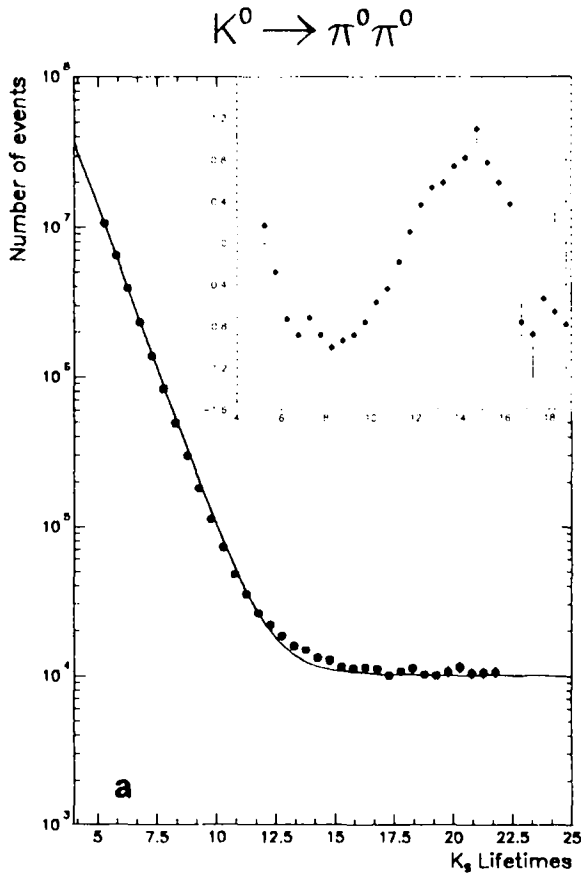


Fig. 5. The rate of decay of kaons to charged and neutral pions as a function of the K_S lifetime. Superimposed are the fitted lifetime distributions with the interference term removed. The insets show the interference terms extracted from the data.

to charged and neutral pions as a function of K_S lifetime, where the K_{near} and K_{far} distributions have been combined. Here the distributions have been summed over momentum and the fitted lifetime distribution with the interference term removed has been superimposed.

The phases of the CP -violating amplitudes are extracted using the following procedure. The ratio of events for K_{near} and K_{far} is calculated in bins of 5 GeV momentum and $0.5\tau_S$ lifetimes. The lifetime is computed for each event from the mid-point between the two targets, in order that the acceptance correction and bin size have the minimum effect on the ratio. Lifetime ranges between 5 and 22.5 K_S lifetimes are also imposed because of the finite decay volume. A simultaneous fit to the charged and neutral ratio distributions is performed. The phases ϕ_{+-} and ϕ_{00} , and a common dilution factor in 10 GeV intervals, are varied in the fit. In addition, a charged and a neutral overall normalization (K_{near}/K_{far}) are allowed to vary separately as a function of momentum and account for variations due to electron rejection and trigger efficiencies. The K_S and K_L lifetimes, the CP -violation parameters η_{+-} and η_{00} , and the mass difference Δm are assumed to be known and fixed to the central values given in table 1. The measured dilution factor $D(p)$ is given in fig. 6. The result of the fit is shown in fig. 7, where all the data have been combined by

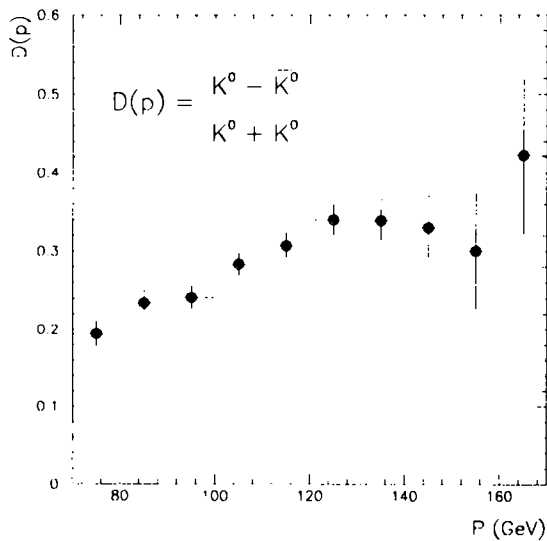


Fig. 6. The dilution factor as a function of K^0 momentum.

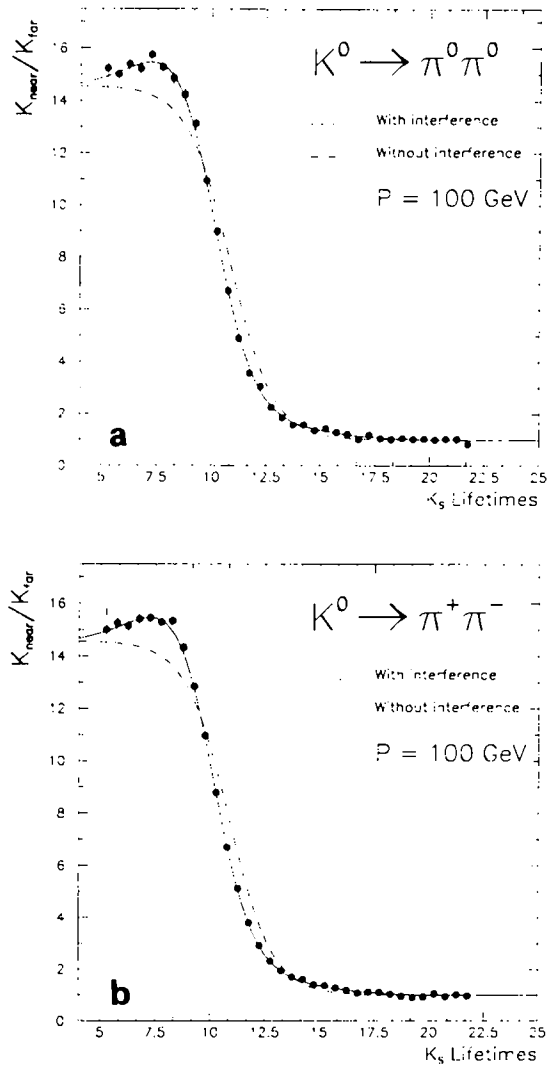


Fig. 7. Ratio distributions averaged over momenta and scaled to 100 GeV. The solid line is the result of the fit with interference; the dashed line is the expectation without interference.

scaling the different momentum bins to 100 GeV.

The various systematic uncertainties in the absolute phases and their difference are listed in table 3 and arise from possible errors in

- the energy scale due to statistical and systematic uncertainties in the K_S anticounter fits, the anticounter efficiency and residual non-linearities;
- the charged and neutral background subtraction procedure;

Table 3
Systematic uncertainties (in degrees).

Contributions	ϕ_{+-}	ϕ_{00}	$\phi_{00}-\phi_{+-}$
energy	0.6	0.8	1.0
non-linearities	0.1	<0.5	<0.5
background	0.1	0.1	0.1
regeneration, scattering	0.1	0.1	-
acceptance	0.1	0.1	0.1
resolution	-	0.2	0.2
mean production point	<0.2	<0.2	-

- additional K^0 production from neutron interactions and regeneration in the collimators and reinteraction in the targets;
- the geometrical acceptance and resolution corrections;
- the position of the K_{near} and K_{far} targets along the beam-line.

Of these, the dominant uncertainty is due to the energy scale.

In addition, there is a dependence of the absolute phases on the assumed values for the K_S lifetime and Δm . The sensitivity of the absolute phases to these parameters is obtained by shifting their central values and refitting. Explicitly, a change in Δm and τ_S affects ϕ_{+-} and ϕ_{00} according to

$$\delta\phi_{+-} = 270^\circ \left(\frac{\tau_S \times 10^{10} \text{s}^{-1} - 0.8922}{0.8922} \right) + 310^\circ \left(\frac{\Delta m \times 10^{-10} \text{s}^{-1} - 0.5351}{0.5351} \right),$$

$$\delta\phi_{00} = 225^\circ \left(\frac{\tau_S \times 10^{10} \text{s}^{-1} - 0.8922}{0.8922} \right) + 310^\circ \left(\frac{\Delta m \times 10^{-10} \text{s}^{-1} - 0.5351}{0.5351} \right).$$

The final result is

$$\phi_{00} - \phi_{+-} = 0.2^\circ \pm 2.6^\circ \pm 1.2^\circ,$$

$$\phi_{+-} = 46.9^\circ \pm 1.4^\circ \pm 0.7^\circ (\pm 0.6^\circ \pm 1.4^\circ),$$

$$\phi_{00} = 47.1^\circ \pm 2.1^\circ \pm 1.0^\circ (\pm 0.5^\circ \pm 1.4^\circ),$$

where the first error is statistical and the second is the quadratic sum of all the systematic uncertainties listed

in table 3. The errors in brackets are due to the current 1 standard deviation uncertainties in τ_S and Δm . The χ^2 per degree of freedom is 796/768 for the simultaneous fit to the charged and neutral distributions. If τ_S and η_{+-} are allowed to vary, the values obtained, $\tau_S = (0.902 \pm 0.005) \times 10^{-10} \text{s}$ and $\eta_{+-} = (2.3 \pm 0.1) \times 10^{-3}$, are consistent within their quoted statistical uncertainties with the values given in table 1.

The phase ϕ_{+-} is in good agreement with previous measurements; ϕ_{00} and $\phi_{00} - \phi_{+-}$ substantially improve the precision previously achieved. Since the phase difference $\phi_{00} - \phi_{+-}$ is consistent with zero, there is no evidence for simultaneous CPT violation in the kaon-state mixing and in the decay. Limits on possible CPT violation in the K^0 mass matrix can be estimated from the magnitude of the parameter δ . In the phenomenology of kaon decay, the component of δ perpendicular to the direction of ϵ can be related to the phases of the CP -violation parameters as follows:

$$\delta_{\perp} \approx |\eta| \left(\frac{2}{3}\phi_{+-} + \frac{1}{3}\phi_{00} - \phi_{\epsilon} \right),$$

assuming $\tau_L \gg \tau_S$ and neglecting CPT violation in the decay amplitudes. Using the values of the phases measured in this experiment, $\frac{2}{3}\phi_{+-} + \frac{1}{3}\phi_{00} = 47.0^\circ \pm 2.0^\circ$ and $\delta_{\perp} = (1.3 \pm 0.8) \times 10^{-4}$. Perturbation theory gives

$$\delta_{\perp} \approx \frac{m_{\bar{K}^0} - m_{K^0}}{2(m_L - m_S)} \sin \phi_{\epsilon}.$$

Thus, using the value of δ_{\perp} extracted above and $m_L - m_S = (3.522 \pm 0.016) \times 10^{-15} \text{ GeV}$, the 95% confidence limit for CPT conservation obtained in this experiment is

$$\left| \frac{m_{\bar{K}^0} - m_{K^0}}{m_{K^0}} \right| < 5 \times 10^{-18}.$$

If the values of the phases obtained in this experiment are combined with previous measurements of ϕ_{+-} (see table 1), the above limit becomes 4×10^{-18} . This limit is now dominated by the absolute phase ϕ_{+-} , which is 1.6 standard deviations from the phase of ϵ and the uncertainty in the mass difference between the short- and long-lived K^0 states.

Acknowledgement

We wish to express our appreciation especially to M. Clément for the technical realization and to G. Dubois for the adaptation of the beam control system to this experiment. We extend our deepest gratitude to F. Blin, G. Fersurella, D. Guyon, G. Juban, G. Laverrière, P. Le Cossec, M. Marin (CERN); D. Brown, A. Main, P. McInnes (Physics Department, University of Edinburgh); K.H. Geib, R. Gläser, A. Weissbeck (Institut für Physik, Universität Mainz); G. Barrand, J.P. Coulon (Linear Accelerator Laboratory, Orsay); S. Galeotti, F. Morsani, L. Zaccarelli (Department of Physics and INFN, University of Pisa), and E. Arik for their dedicated efforts in the operation of the experiment. We acknowledge support from the SERC and Rutherford Appleton Laboratory.

References

- [1] M. Kobayashi and K. Maskawa, *Prog. Theor. Phys.* 49 (1973) 652.
- [2] J. Ellis, M.K. Gaillard and D.V. Nanopoulos, *Nucl. Phys. B* 109 (1976) 213.
- [3] G. Lüders, *Ann. Phys.* 2 (1957) 1.
- [4] W. Pauli, Niels Bohr and the development of physics (Pergamon, London, 1955).
- [5] K.R. Schubert et al., *Phys. Lett. B* 31 (1970) 662.
- [6] V.V. Barmin et al., *Nucl. Phys. B* 247 (1984) 293.
- [7] M. Cullen et al., *Phys. Lett. B* 32 (1970) 523;
S. Gjesdal et al., *Phys. Lett. B* 52 (1974) 113;
C. Geweniger et al., *Phys. Lett. B* 52 (1974) 108.
- [8] T.D. Lee and C.S. Wu, *Annu. Rev. Nucl. Sci.* 16 (1966) 511.
- [9] T.T. Wu and C.N. Yang, *Phys. Rev. Lett.* 13 (1964) 380.
- [10] J.S. Bell and J. Steinberger, *Proc. Intern. Conf. on Elementary Particles* (Oxford, 1965) (Rutherford Laboratory, Didcot, 1966) p. 195.
- [11] H. Burkhardt et al., *Phys. Lett. B* 206 (1988) 169.
- [12] K. Kleinknecht, *Annu. Rev. Nucl. Sci.* 26 (1976) 1;
T.T. Devlin and J.O. Dickey, *Rev. Mod. Phys.* 51 (1979) 237;
N.N. Biswas et al., *Phys. Rev. Lett.* 47 (1981) 1378;
A.N. Kamal, *J. Phys. G* 12 (1986) L43;
H.Y. Cheng, *Phys. Lett. B* 201 (1988) 155.
- [13] C. Geweniger et al., *Phys. Lett. B* 48 (1974) 487.
- [14] S. Gjesdal et al., *Phys. Lett. B* 52 (1974) 119.
- [15] J.H. Christenson et al., *Phys. Rev. Lett.* 43 (1979) 1212.
- [16] R. Messner et al., *Phys. Rev. Lett.* 30 (1973) 876;
R. DeVoe et al., *Phys. Rev. D* 16 (1977) 565;
D.P. Coupal et al., *Phys. Rev. Lett.* 55 (1985) 566.
- [17] M. Woods et al., *Phys. Rev. Lett.* 60 (1988) 1695.
- [18] W.C. Carithers et al., *Phys. Rev. Lett.* 34 (1975) 1244.
- [19] J.H. Christenson et al., *Phys. Rev. Lett.* 43 (1979) 1209.
- [20] O. Skjeggstad et al., *Nucl. Phys. B* 48 (1972) 343;
S. Aronson et al., *Nuovo Cimento* 32A (1976) 236.
P. Grossmann et al., *Phys. Rev. Lett.* 59 (1987) 18.
- [21] K.G. Vosburgh et al., *Phys. Rev. D* 6 (1972) 1834.
- [22] H. Burkhardt et al., *Nucl. Instrum. Methods A* 268 (1988) 116.
- [23] H. Burkhardt et al., *Phys. Lett. B* 199 (1987) 139.